FEBS Letters 583 (2009) 897–902

FEBS Letters

journal homepage: www.FEBSLetters.org

Release of extracellular membrane vesicles from microvilli of epithelial cells is enhanced by depleting membrane cholesterol

Anne-Marie Marzesco [a], Michaela Wilsch-Bräuninger [a], Véronique Dubreuil [a,1], Peggy Janich [b], Katja Langenfeld [a], Christoph Thiele [a], Wieland B. Huttner [a,*], Denis Corbeil [b,*]

[a] Max-Planck-Institute of Molecular Cell Biology and Genetics, Pfotenhauerstrasse 108, 01307 Dresden, Germany
[b] Tissue Engineering Laboratories, BIOTEC and DFG Research Center and Cluster of Excellence for Regenerative Therapies Dresden (CRTD), Technische Universität Dresden, Tatzberg 47-49, 01307 Dresden, Germany

ARTICLE INFO

Article history:
Received 28 November 2008
Revised 24 January 2009
Accepted 27 January 2009
Available online 31 January 2009

Edited by Sandro Sonnino

Keywords:
Prominin
CD133
Cholesterol
Microvilli
Epithelial cell
Cancer

ABSTRACT

We previously reported on the occurrence of prominin-1-carrying membrane vesicles that are released into body fluids from microvilli of epithelial cells. This release has been implicated in cell differentiation. Here we have characterized these vesicles released from the differentiated Caco-2 cells. We find that in these vesicles, prominin-1 directly interacts with membrane cholesterol and is associated with a membrane microdomain. The cholesterol depletion using methyl-β-cyclodextrin resulted in a marked increase in their release, and a dramatic change in the microvillar ultrastructure from a tubular shape to a "pearling" state, with multiple membrane constrictions, suggesting a role of membrane cholesterol in vesicle release from microvilli.

1. Introduction

Whereas intracellular membrane traffic has been extensively investigated, less is known about membrane particles released from cells. By far the most frequently studied extracellular vesicles are exosomes [1]. However, recent studies have revealed an increasing diversity of extracellular particles, not only in terms of their type but also with regard to their origin [2–4]. We previously reported on a novel class of membrane vesicles that was identified in the ventricular fluid of the embryonic mouse brain [3,4]. These small (50–80 nm) electron-translucent vesicles appear to have a widespread distribution, being found not only in the embryonic and adult cerebrospinal fluid [3,5], but also in various external body fluids, including saliva [3,6]. Their sites of origin appear to be microvilli and primary cilia [3,4,6]. A marker in the characterization of these vesicles is prominin-1 (CD133), a membrane glycoprotein expressed by epithelial and non-epithelial cells including various stem/cancer stem cells [7–10]. Prominin-1 exhibits a preference for plasma membrane protrusions, e.g. microvilli [3,4,6,7,11], and its accumulation therein reflects its association with a cholesterol-based membrane microdomain [12,13]. This association is presumably mediated by its ability to directly interact with membrane cholesterol [12].

Little is known about the mechanism underlying the release of the extracellular prominin-1-containing membrane vesicles (PMVs) from their presumptive donor membranes. Several lines of evidence suggest a link between this release and cell differentiation/dedifferentiation. Thus, the PMVs increase in the ventricular fluid of the embryonic mouse brain during neurogenesis [3], and decrease in human patients with glioblastoma during the final phase of the disease [5]. In a cell culture model, the human colon-carcinoma-derived Caco-2 cells in which prominin-1 is specifically localized in the microvilli [11], we demonstrated that the PMVs are increasingly released upon their differentiation [3].

In intracellular membrane traffic, the formation of cytoplasmic vesicles from the plasma membrane is controlled not only by the protein machinery, but also by lipids, notably cholesterol [14–17]. Given the cholesterol-binding capacity of prominin-1 and its association with a membrane microdomain, it was of interest to explore the possibility whether the release of the PMVs from microvilli is affected by membrane cholesterol level.

* Corresponding authors. Fax: +49 (0) 351 463 40244 (D. Corbeil), +49 (0) 351 210 1600 (W.B. Huttner).
E-mail addresses: huttner@mpi-cbg.de (W.B. Huttner), corbeil@biotec.tu-dresden.de (D. Co.
[1] Present address: UMR 8542, CNRS, Ecole Normale Supérieure, 46, rue d'Ulm, F-75005 Paris, France.

0014-5793/$34.00 © 2009 Federation of European Biochemical Societies. Published by Elsevier B.V. All rights reserved.
doi:10.1016/j.febslet.2009.01.048

2. Materials and methods

2.1. Cell culture

Caco-2 cells (ATCC® HTB-37) were grown as described [3], except that Dulbecco's minimal essential medium (DMEM) supplemented with 10% fetal calf serum (FCS), 1% non-essential amino acids (Life Technologies Inc., Paisley, UK), 2 mM L-glutamine, 100 U/ml penicillin, and 100 μg/ml streptomycin (complete medium) was used.

2.2. Cholesterol depletion

Caco-2 cells grown for 10 days post-confluency (dpc) were treated for 48 h according the following conditions. Cells received for 24 h either 1.5 ml of complete medium or medium supplemented with 10% delipidated FCS [18] with or without 10 μM Lovastatin sodium (Calbiochem, #438186). After 24 h, media were discarded and cells were incubated for an additional 24 h with either 1.5 ml of complete medium or medium supplemented with 10% delipidated FCS with or without 10 μM Lovastatin sodium and with or without 2 mM methyl-β-cyclodextrin (mβCD; Sigma). After 24 h, collected media were subjected to centrifugation at 4 °C for 30 min at 10000×*g* and the resulting supernatants for 1 h at 110000×*g*. The 110000×*g*-pellets were dissolved in SDS sample buffer. Cells were washed with PBS and lysed directly in SDS sample buffer.

2.3. Detergent resistance

Differentiated Caco-2 cells received 5 ml of complete medium, which was collected after 24 h. The conditioned medium was divided and subjected to differential centrifugation at 4 °C as follows: 30 min at 10000×*g*, supernatant 1 hr at 200000×*g*. The resulting 200000×*g*-pellets were resuspended either in 50 μl PBS or PBS containing 10 mM mβCD, and incubated for 30 min at 37 °C. Samples were then mixed with PBS containing either 1% Triton X-100 (Sigma) or 1% Lubrol WX (SERVA) and incubated for 30 min at 4 °C, before a centrifugation for 1 hr at 100000×*g* at 4 °C. The supernatants and pellets were analyzed by immunoblotting.

2.4. SDS–PAGE and immunoblotting

SDS–PAGE followed by immunoblotting were performed [19] using either rabbit antiserum αhE2 against prominin-1 [20] or anti-α-tubulin mouse monoclonal antibody (clone DM1A; Sigma). Chemiluminescence (ECL system, Amersham Biosciences) was recorded using a cooled CCD camera (Fujifilm LAS 1000 Imaging system, Fuji Photo Film) and Image Reader Pro Ver2.01 software. Quantification was performed using Image Gauge V3.3 software.

2.5. Photo-cholesterol labeling and immunoprecipitation

Photocholesterol labeling using a [^{3}H]photocholesterol-mβCD inclusion complex [18] was performed as described [12]. Labeling was performed with PMVs found either in Caco-2 medium or saliva.

2.5.1. Caco-2 medium

Differentiated Caco-2 cells received serum-free medium (Opti-MEM, Gibco) supplemented as above. After 24 h, the conditioned medium was centrifuged for 30 min at 10000×*g* and the supernatant (30 ml) concentrated to 10 ml using Centricon plus-20 (Millipore). Concentrated medium was incubated with 400 μCi [^{3}H]photocholesterol-mβCD complex for 2 h at 37 °C. Nine milliliter of the medium were then transferred onto a 150-mm dish on ice and irradiated with UV-light for 5 min whereas the remaining 1 ml was kept in the dark (negative control). One milliliter of irradiated sample and the negative control were subjected to centrifugation at 4 °C for 2 h at 110000×*g*. The pellets and the methanol/chloroform-precipitated material recovered from the supernatants were dissolved in SDS-sample buffer. The remaining 8 ml of UV-irradiated medium was incubated for 1 h at 4 °C with 2 ml of ice-cold (5×) RIPA buffer [6]. Two 5 ml aliquots were incubated for 1 h at 4 °C with either 10 μl of antiserum αhE2 or 50 μg of rabbit IgG. Immune-complexes were pulled-down using Protein G-Sepharose 4 matrix (Amersham Biosciences, Uppsala, Sweden) overnight at 4 °C, washed with RIPA buffer, and dissolved in SDS sample buffer. Samples were analyzed by SDS–PAGE followed by fluorography [12].

2.5.2. Saliva

Saliva (2 ml) obtained from healthy volunteers was mixed with 2 ml of ice-cold PBS, filtered through cotton gauze, and centrifuged at 4 °C for 30 min at 10000×*g*. The supernatant was incubated at 37 °C for 3 h with 80 μCi of [^{3}H]photocholesterol-mβCD complex. Half of the sample was kept in the dark and the other half irradiated with UV-light for 5 min. Samples were centrifuged at 4 °C for 1 h at 200000×*g*. The pellet was resuspended in 600 μl of RIPA buffer. Prominin-1 was immunoprecipitated from an aliquot (500 μl) using antiserum αhE2. Immunoprecipitates and the remaining 100 μl (resuspended pellet) were analyzed by fluorography.

2.6. Electron microscopy

Caco-2 cells grown for 10–12 dpc on permeable filters (Costar, Cambridge, Mass) were subjected to various conditions as described above. Cells were processed for standard electron microscopy [3], and samples examined with a Morgagni electron microscope (FEI company, Eindhoven, NL).

3. Results

3.1. Extracellular vesicle-associated prominin-1 interacts with membrane cholesterol

It was previously shown that prominin-1 concentrated in microvilli of epithelial cells directly interacts with membrane cholesterol [12]. Given this finding, and that the PMVs apparently originate from microvilli [3], we investigated whether the vesicle-associated prominin-1 also interacts with cholesterol. The PMVs released from differentiated Caco-2 cells in complete medium were incubated with [^{3}H]photocholesterol [18], followed by UV-irradiation and immunoprecipitation of prominin-1. This revealed covalent binding of [^{3}H]photocholesterol to vesicle-associated prominin-1 (Fig. 1a, lane 6). Specificity of the labeling was documented by (i) the dependence on UV-irradiation (Fig. 1a, lanes 2 and 4 versus 1 and 3), (ii) the labeling of apolipoproteins A1 and B (Fig. 1a, lane 2, thick arrows), two cholesterol-binding proteins, and (iii) the distinct pattern of [^{3}H]photocholesterol-labeled bands as compared to the protein staining (Fig. 1a, lane 5).

We performed a similar experiment with saliva, a physiological fluid known to contain PMVs [3]. The immunoprecipitation of prominin-1 revealed its covalent binding of [^{3}H]photocholesterol (Fig. 1b, lane 3).

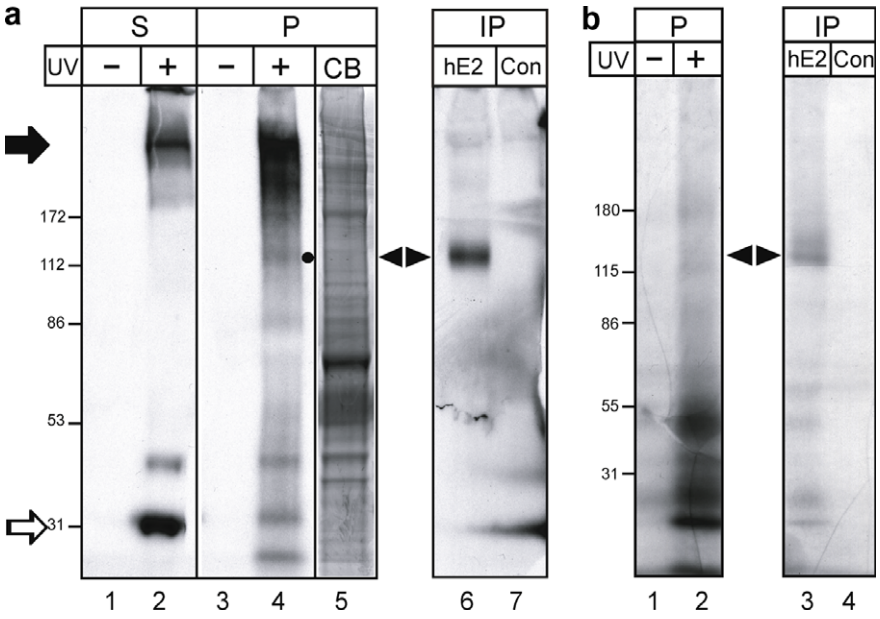

Fig. 1. Membrane vesicles-associated prominin-1 interacts directly with membrane cholesterol. The 24 h-conditioned medium of Caco-2 cells (a) or human saliva (b) was incubated with [^{3}H]photocholesterol-mβCD complex and subjected to UV irradiation (+) or without (−). The saliva and an aliquot of the medium were ultracentrifuged to obtain pellet (P) and supernatant (S). Prominin-1 was immunoprecipitated (IP) from the remainder of the UV-irradiated medium and from an aliquot of the UV-irradiated saliva pellet, using the antiserum αhE2 (hE2) or, as control, rabbit IgG (con). Supernatants, pellets and immunoprecipitates were analyzed by fluorography. For comparison, lane 5 shows the Coomassie Blue (CB) staining of the pellet obtained from the UV-irradiated Caco-2 medium. Arrowheads and solid circle, prominin-1 or position where prominin-1 would be expected; solid arrow, apolipoprotein B; open arrow, apolipoprotein A1.

3.2. Prominin-1 in extracellular membrane vesicles is associated with a specific membrane microdomain

Within microvilli, prominin-1 is associated with a cholesterol-dependent membrane microdomain that is recovered in the non-ionic detergent Lubrol WX but solubilized in Triton X-100 [12]. Given this finding and the interaction of vesicle-associated prominin-1 with membrane cholesterol (Fig. 1), we investigated whether the vesicle-associated prominin-1 would also be found with a similar membrane microdomain. Indeed, the vesicle-associated prominin-1 released from differentiated Caco-2 cells (Supplementary Fig. S1, lane 1, in Supplementary data) was recovered as detergent-resistant membrane when using Lubrol WX (Supplementary Fig. S1 top, lane 5), but not Triton X-100 (Supplementary Fig. S1, lanes 3 and 4). This reflected the existence of a cholesterol-dependent membrane microdomain, as prior cholesterol extraction from the membrane vesicles by the cholesterol sequestering agent mβCD resulted in the almost complete solubilization of prominin-1 in Lubrol WX (Supplementary Fig. S1 bottom, lanes 5 and 6).

3.3. Extraction of plasma membrane cholesterol promotes the release of PMVs

We explored next whether the appearance of the PMVs [3] is affected by changes in the cholesterol level. Specifically, we pre-treated differentiated Caco-2 cells for 24 h by incubation in various media predicted to lower cellular cholesterol, and then extracted membrane cholesterol by incubation of cells for an additional 24 h with mβCD, as specified (Fig. 2a). PMVs present in the second 24 h conditioned medium were analyzed by immunoblotting of the pellet obtained after ultracentrifugation.

Incubation of cells with complete medium containing 2 mM mβCD (condition 4) resulted in a twofold ($P < 0.015$) increase in vesicle-associated prominin-1 in the medium compared to incubation with complete medium without mβCD (condition 1) (Fig. 2c). This effect was enhanced when the mβCD treatment was performed on cells in which cholesterol supply and biosynthesis had been reduced by use of delipidated serum and addition of 10 μM Lovastatin, respectively (condition 6) (Fig. 2b and c). The increase in vesicle-associated prominin-1 in the medium upon cholesterol extraction was matched by a decrease in cell-associated prominin-1 (Fig. 2b). Reduction of cholesterol supply and biosynthesis alone (condition 3) did not cause an increase in vesicle-associated prominin-1 (Fig. 2c). To exclude that the increase in vesicle-associated prominin-1 in the medium reflected a general fragmentation of the plasma membrane, we examined the α-tubulin content of the cells after the various treatments. No loss of α-tubulin was detected in any condition (Fig. 2d). These data suggested that extraction of cholesterol from the plasma membrane promoted the release of PMVs. Finally, it is important to note that under our experimental conditions, particularly those involving mβCD, no significant cell death could be observed (data not shown). Together with the lack of cellular loss of α-tubulin, this suggested that the effect of mβCD on PMV release was not due to a cytotoxic effect of the drug.

3.4. Morphology of microvilli upon cholesterol depletion

These observations prompted us to investigate the morphology of the microvilli of cholesterol-extracted Caco-2 cells. Electron microscopy of cells grown in complete medium revealed a typical brush border with densely packed microvilli (Fig. 3a). It should be noted that their length was not uniform throughout the cell monolayer but varied between cells, although for any given single cell most microvilli had a similar length (Fig. 3a; however, note panel c). Occasionally, we observed membrane constrictions close to the tip of microvilli of cells grown in complete medium (Fig. 3b, c, arrowheads). Incubation of cells in medium containing delipidated serum and 10 μM Lovastatin did not significantly alter their architecture (Fig. 3d).

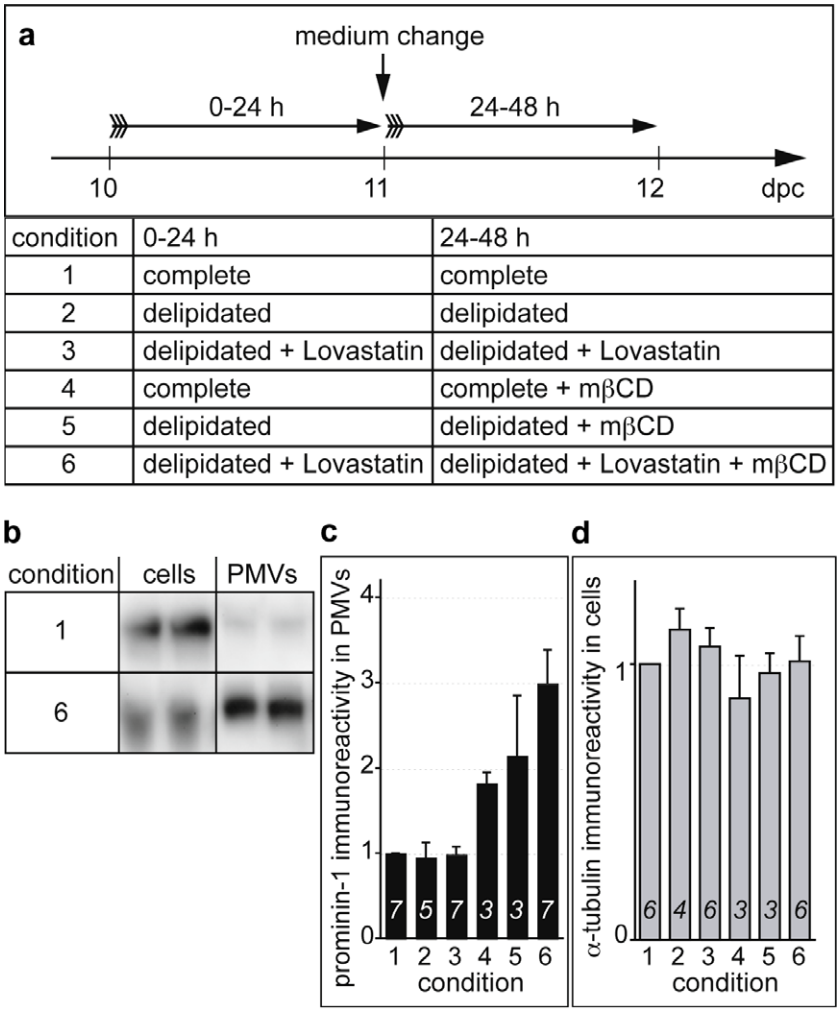

condition	0-24 h	24-48 h
1	complete	complete
2	delipidated	delipidated
3	delipidated + Lovastatin	delipidated + Lovastatin
4	complete	complete + mβCD
5	delipidated	delipidated + mβCD
6	delipidated + Lovastatin	delipidated + Lovastatin + mβCD

Fig. 2. Cholesterol depletion promotes the release of PMVs. (a) Summary of the different conditions. Caco-2 cells grown for 10 dpc in complete medium were exposed to various media for 0–24 h and 24–48 h, as indicated: complete medium (complete); complete with delipidated FCS instead of FCS (delipidated); complete with delipidated FCS plus 10 μM Lovastatin (delipidated + Lovastatin); complete with 2 mM mβCD (complete + mβCD); complete with delipidated FCS plus 2 mM mβCD (delipidated + mβCD); complete with delipidated FCS plus 10 μM Lovastatin and 2 mM mβCD (delipidated + Lovastatin + mβCD). (b) The 24–48 h medium obtained in the various conditions (a) was centrifuged at 10000×*g*, and the resulting supernatant at 110000×*g* to sediment the PMVs. An aliquot (1/3) of this pellet and of the corresponding cells (1/30) were analyzed by immunoblotting for prominin-1. (c and d) Quantification of immunoblots obtained in the various conditions. (c) Prominin-1 immunoreactivity in PMVs was determined as a percentage of total (sum of PMV + cells), and the resulting values are expressed relative to that of condition 1 (5%), which was arbitrarily set to 1. (d) α-Tubulin immunoreactivity associated with cells is expressed relative to that of condition 1 (arbitrarily set to 1). Numerals in the column bars indicate the number of independent experiments, each performed in triplicate; column bars show the mean of the independent experiments, error bars indicate S.E.M.

In contrast, extraction of cholesterol with mβCD resulted in dramatic changes in microvillar ultrastructure (Fig. 3k), particularly when this treatment was performed in medium reducing the supply of cholesterol (delipidated serum, Fig. 3l) and inhibiting its biosynthesis (Lovastatin, Fig. 3e–j). The magnitude of the effect of cholesterol extraction varied between cells, but for the microvilli of any given single cell was very similar. Specifically, we observed that (i) a brush border was only maintained in rare cases (Fig. 3e), (ii) the number and length of microvilli was drastically reduced (Fig. 3j and l), and (iii) their shape often appeared irregular, with membrane constrictions at their tips (Fig. 3f, k, arrowheads) or throughout their entire length (Fig. 3g, i, k, arrowheads) as the most distinctive feature. In the latter cases, the appearance of the microvilli was reminiscent of the previously described "pearling" of tubular cell protrusions and artificial lipid bilayers [21–24].

In addition to this "pearling" of microvilli, there was a striking appearance of small membrane vesicles in the immediate vicinity of the microvilli (Fig. 3e, f, I, and k), as has previously been observed upon cholesterol depletion of enterocytes [25]. The size of these vesicles was very similar to that of the individual "pearl"-like units of the cholesterol-depleted microvilli, suggesting that the latter were the precursors to the former. Another morphological change elicited by cholesterol extraction was the marked increase in aggregated granular electron-dense material at the microvillar tip (Fig. 3h, open arrow). Besides the changes in brush border morphology, we noticed an increase in the occurrence of intracellular multivesicular structures upon extraction of membrane cholesterol by mβCD (Supplementary Fig. S2 in Supplementary data), in line with previous observations [25].

4. Discussion

The release of PMVs from microvilli into extracellular fluids is a widespread phenomenon. However, the underlying mechanism is unclear. Using prominin-1, we show that the released PMVs are indistinguishable from their donor membranes with regard to microdomain organization. Thus, the vesicle-associated prominin-1 showed the same differential solubility/insolubility in Triton X-100 versus Lubrol WX, and specific interaction with membrane

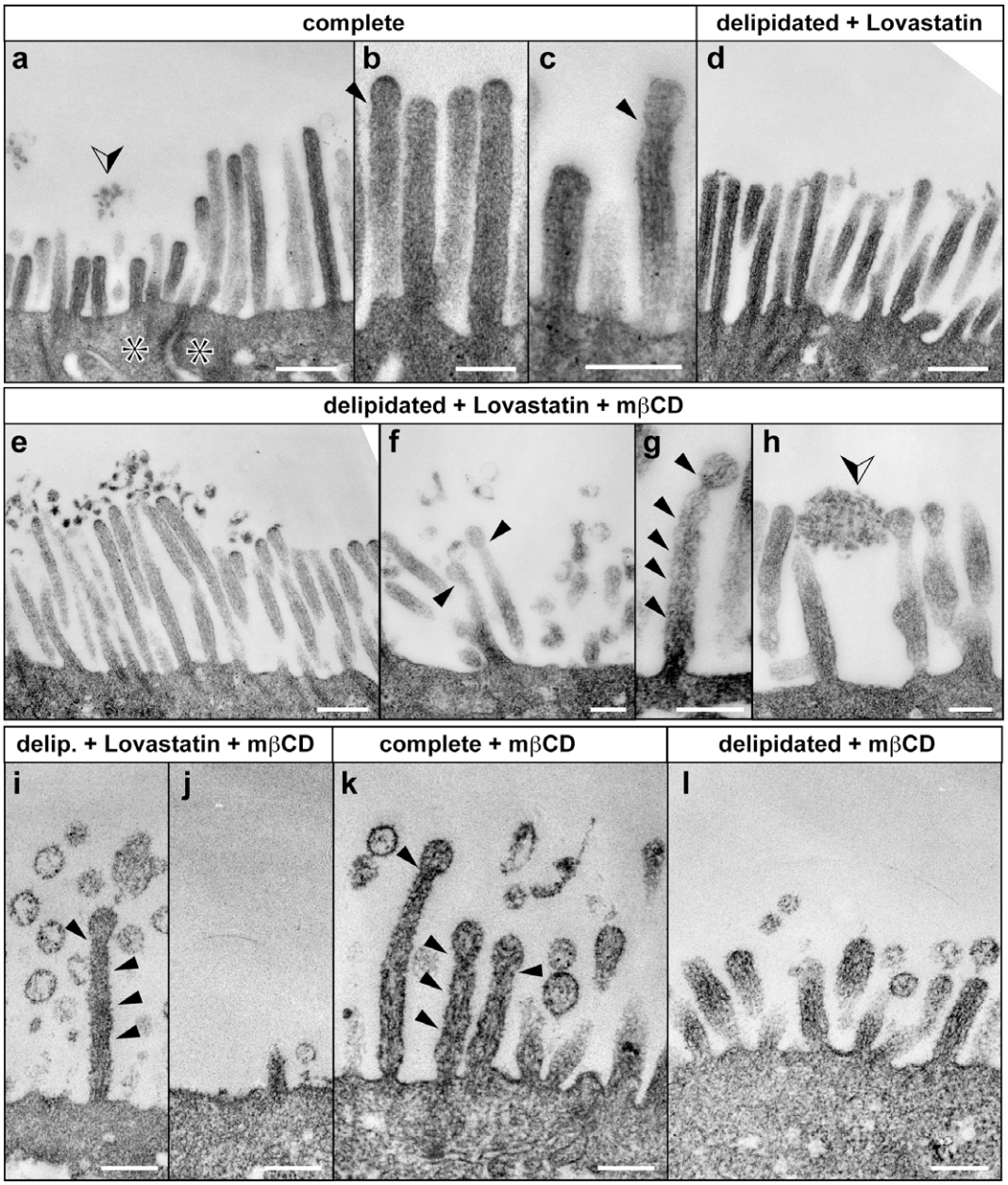

Fig. 3. Electron microscopic analysis of microvilli of cholesterol-depleted cells. Caco-2 cells grown for 10 (b, i–l) or 12 (a, c–h) dpc were exposed to various media as in Fig. 2a; labeling above panels refers to the 24–48 h period. (a–c) Condition 1; (d) condition 3; (e–j) condition 6; (k) condition 4; (l) condition 5. Asterisks in (a) flank junctional complexes of two adjacent cells; note the difference in microvillar length in these cells grown in complete medium. Arrowheads, membrane constrictions; note that these are confined to the microvillar tip in complete medium (b, c) and are increasingly observed upon the mβCD treatment (f, g, i, k). Open arrows, aggregated granular electron-dense material in the vicinity of microvilli. Bars: a, d, e, 400 nm; b, c, f–l, 200 nm.

cholesterol, as previously reported for prominin-1 in microvilli [12].

As to the cell biological mechanism underlying the release of PMVs, our study suggests that changes in membrane microdomain organization can affect it. Specifically, cholesterol depletion, which has previously been shown to reduce the size of the prominin-1–containing membrane microdomain [12], was found to cause a marked increase in the release of PMVs. At the level of the donor membrane, the morphological correlate of the increased vesicle release upon cholesterol depletion was a transition in the microvillar structure from a tubular shape to a "pearling" state, with multiple membrane constrictions all along their length (Supplementary Fig. S3 in Supplementary data). When microvilli showed only single membrane constrictions, these were typically found near their tips, suggesting that these were the sites where pearling was initiated. Pearling of tubular cell membranes and lipid bilayer tubes has previously been shown to reflect the balance of two competing parameters, curvature and tension [22–24]. In the case of tubular plasma membrane protrusions, tension is exerted, at least in part, by the actin cytoskeleton, depolymerization of which (and hence lowering tension) leads to pearling [22]. The transition from a tubular shape to a pearling state upon cholesterol depletion observed here, however, is presumably due to increasing curvature, as tubular membranes exhibit curvature only in two dimensions whereas pearling membranes do so in three dimensions. Our demonstration that cholesterol depletion, which is known to affect curvature [26–29], causes pearling of microvilli, is consistent with previous studies on artificial lipid bilayers [23,30].

Is the influence of membrane cholesterol levels on the occurrence of pearling and on the extent of PMVs release physiologically relevant? It is interesting to note that pearling of microvilli and the presence of vesicles between microvilli have been observed in the duodenal brush border of chicks receiving a low residue diet [21], suggesting that pearling is a physiological intermediate in the release of vesicles from microvilli. Moreover, the differentiation of Caco-2 cells that occurs post-confluency and that is associated with an increase in the release of PMVs [3] is accompanied by a decrease in membrane cholesterol levels [31]. Together with the induction of vesicle fission from artificial lipid bilayer tubes upon cholesterol removal [24], these observations are consistent with the possibility that the budding and fission of vesicles from microvilli into extracellular fluids is controlled, at least in part, by the level of membrane cholesterol and the cholesterol-dependent organization of membrane microdomains. Given that the induction of vesicle fission from artificial lipid bilayer tubes upon cholesterol removal is thought to involve phase separation [24], the pearling of microvilli and increased vesicle release therefrom may also reflect phase separation. In this context, it should be considered that the pearling of microvilli observed upon interference with the intramicrovillar actomyosin system [32] may reflect phase separation resulting from the clustering of small membrane microdomains into larger ones. Taken the previous [33,34] and present studies together, regulating the interplay between cholesterol-dependent membrane microdomains and the membrane-associated actomyosin system emerges as a potential mechanism controlling the physiological release of microvilli-derived membrane vesicles. Given that this release has been implicated in cell differentiation, our data suggest a new role of cholesterol-dependent membrane microdomains in cell differentiation.

Acknowledgements

C.T. was supported by Deutsche Forschungsgemeinschaft (DFG; SFB/TR13-04.D2), W.B.H. by the DFG (SPP 1109, Hu275/7-3; SPP 1111, Hu275/8-3; SFB/TR13-04.B1; SFB 655.A2) and D.C. by the DFG (SPP 1109, CO298/2-2; SFB/TR13-04.B1; SFB 655.A13) and Sächsisches Ministerium für Wissenschaft und Kunst-Europäischer Fond für Regionale Entwicklung (4212/05-16).

Appendix A. Supplementary data

Supplementary data associated with this article can be found, in the online version, at doi:10.1016/j.febslet.2009.01.048.

References

[1] Lakkaraju, A. and Rodriguez-Boulan, E. (2008) Itinerant exosomes: emerging roles in cell and tissue polarity. Trends Cell. Biol. 18, 199–209.
[2] Bachy, I., Kozyraki, R. and Wassef, M. (2008) The particles of the embryonic cerebrospinal fluid: how could they influence brain development? Brain Res. Bull. 75, 289–294.
[3] Marzesco, A.M., Janich, P., Wilsch-Brauninger, M., Dubreuil, V., Langenfeld, K., Corbeil, D. and Huttner, W.B. (2005) Release of extracellular membrane particles carrying the stem cell marker prominin-1 (CD133) from neural progenitors and other epithelial cells. J. Cell Sci. 118, 2849–2858.
[4] Dubreuil, V., Marzesco, A.M., Corbeil, D., Huttner, W.B. and Wilsch-Brauninger, M. (2007) Midbody and primary cilium of neural progenitors release extracellular membrane particles enriched in the stem cell marker prominin-1. J. Cell Biol. 176, 483–495.
[5] Huttner, H.B. et al. (2008) The stem cell marker prominin-1/CD133 on membrane particles in human cerebrospinal fluid offers novel approaches for studying central nervous system disease. Stem Cells 26, 698–705.
[6] Florek, M. et al. (2007) Prominin-2 is a cholesterol-binding protein associated with apical and basolateral plasmalemmal protrusions in polarized epithelial cells and released into urine. Cell Tissue Res. 328, 31–47.
[7] Weigmann, A., Corbeil, D., Hellwig, A. and Huttner, W.B. (1997) Prominin, a novel microvilli-specific polytopic membrane protein of the apical surface of epithelial cells, is targeted to plasmalemmal protrusions of non-epithelial cells. Proc. Natl. Acad. Sci. USA 94, 12425–12430.
[8] Yin, A.H. et al. (1997) AC133, a novel marker for human hematopoietic stem and progenitor cells. Blood 90, 5002–5012.
[9] Fargeas, C.A., Fonseca, A.-V., Huttner, W.B. and Corbeil, D. (2006) Prominin-1 (CD133): from progenitor cells to human diseases. Future Lipidol. 1, 213–225.
[10] Karbanová, J. et al. (2008) The stem cell marker CD133 (Prominin-1) is expressed in various human glandular epithelia. J. Histochem. Cytochem. 56, 977–993.
[11] Corbeil, D. et al. (2000) The human AC133 hematopoietic stem cell antigen is also expressed in epithelial cells and targeted to plasma membrane protrusions. J. Biol. Chem. 275, 5512–5520.
[12] Röper, K., Corbeil, D. and Huttner, W.B. (2000) Retention of prominin in microvilli reveals distinct cholesterol-based lipid microdomains in the apical plasma membrane. Nat. Cell Biol. 2, 582–592.
[13] Janich, P. and Corbeil, D. (2007) GM1 and GM3 gangliosides highlight distinct lipid microdomains within the apical domain of epithelial cells. FEBS Lett. 581, 1783–1787.
[14] Wang, Y., Thiele, C. and Huttner, W.B. (2000) Cholesterol is required for the formation of regulated and constitutive secretory vesicles from the trans-Golgi network. Traffic 1, 952–962.
[15] Schmidt, K., Schrader, M., Kern, H.-F. and Kleene, R. (2001) Regulated apical secretion of zymogens in rat pancreas. Involvement of the glycosylphosphatidylinositol-anchored glycoprotein GP-2, the lectin ZG16p, and cholesterol–glycosphingolipid-enriched microdomains. J. Biol. Chem. 276, 14315–14323.
[16] Rodal, S.K., Skretting, G., Garred, O., Vilhardt, F., van Deurs, B. and Sandvig, K. (1999) Extraction of cholesterol with methyl-b-cyclodextrin perturbs formation of clathrin-coated endocytic vesicles. Mol. Biol. Cell 10, 961–974.
[17] Subtil, A., Gaidarov, I., Kobylarz, K., Lampson, M.A., Keen, J.H. and McGraw, T.E. (1999) Acute cholesterol depletion inhibits clathrin-coated pit budding. Proc. Natl. Acad. Sci. USA 96, 6775–6780.
[18] Thiele, C., Hannah, M.J., Fahrenholz, F. and Huttner, W.B. (2000) Cholesterol binds to synaptophysin and is required for biogenesis of synaptic vesicles. Nat. Cell Biol. 2, 42–49.
[19] Corbeil, D., Fargeas, C.A. and Huttner, W.B. (2001) Rat prominin, like its mouse and human orthologues, is a pentaspan membrane glycoprotein. Biochem. Biophys. Res. Commun. 285, 939–944.
[20] Florek, M., Haase, M., Marzesco, A.M., Freund, D., Ehninger, G., Huttner, W.B. and Corbeil, D. (2005) Prominin-1/CD133, a neural and hematopoietic stem cell marker, is expressed in adult human differentiated cells and certain types of kidney cancer. Cell Tissue Res. 319, 15–26.
[21] Hobbs, D.G. (1980) The origin and distribution of membrane-bound vesicles associated with the brush border of chick intestinal mucosa. J. Anat. 131, 635–642.
[22] Bar-Ziv, R., Tlusty, T., Moses, E., Safran, S.A. and Bershadsky, A. (1999) Pearling in cells: a clue to understanding cell shape. Proc. Natl. Acad. Sci. USA 96, 10140–10145.
[23] Baumgart, T., Hess, S.T. and Webb, W.W. (2003) Imaging coexisting fluid domains in biomembrane models coupling curvature and line tension. Nature 425, 821–824.
[24] Roux, A., Cuvelier, D., Nassoy, P., Prost, J., Bassereau, P. and Goud, B. (2005) Role of curvature and phase transition in lipid sorting and fission of membrane tubules. EMBO J. 24, 1537–1545.
[25] Hansen, G.H., Niels-Christiansen, L.L., Thorsen, E., Immerdal, L. and Danielsen, E.M. (2000) Cholesterol depletion of enterocytes. Effect on the Golgi complex and apical membrane trafficking. J. Biol. Chem. 275, 5136–5142.
[26] Needham, D. and Nunn, R.S. (1990) Elastic-deformation and failure of lipid bilayer-membranes containing cholesterol. Biophys. J. 58, 997–1009.
[27] Evans, E. and Rawicz, W. (1990) Entropy-driven tension and bending elasticity in condensed-fluid membranes. Phys. Rev. Lett. 64, 2094–2097.
[28] Chen, Z. and Rand, R. (1997) The influence of cholesterol on phospholipid membrane curvature and bending elasticity. Biophys. J. 73, 267–276.
[29] Wang, W., Yang, L. and Huang, H.W. (2007) Evidence of cholesterol accumulated in high curvature regions: implication to the curvature elastic energy for lipid mixtures. Biophys. J. 92, 2819–2830.
[30] Yanagisawa, M., Imai, M. and Taniguchi, T. (2008) Shape deformation of ternary vesicles coupled with phase separation. Phys. Rev. Lett. 100, 148102-1–148102-4.
[31] Jindrichova, S., Novakova, O., Bryndova, J., Tvrzicka, E., Lisa, V., Novak, F. and Pacha, J. (2003) Corticosteroid effect on Caco-2 cell lipids depends on cell differentiation. J. Steroid Biochem. Mol. Biol. 87, 157–165.
[32] Tyska, M.J., Mackey, A.T., Huang, J.-D., Copeland, N.G., Jenkins, N.A. and Mooseker, M.S. (2005) Myosin-1a is critical for normal brush border structure and composition. Mol. Biol. Cell 16, 2443–2457.
[33] Tyska, M.J. and Mooseker, M.S. (2004) A role for myosin-1A in the localization of a brush border disaccharidase. J. Cell Biol. 165, 395–405.
[34] McConnell, R.E. and Tyska, M.J. (2007) Myosin-1a powers the sliding of apical membrane along microvillar actin bundles. J. Cell Biol. 177, 671–681.